論文 / 著書情報
Article / Book Information

Title	Fabrication and characterization of perovskite solar cells added with MnCl2, YCl3 or poly(methyl methacrylate)
Authors	Masaya Taguchi, Atsushi Suzuki, Hiroki Tanaka, Takeo Oku
Citation	AIP Conference Proceedings, Vol. 1929, 1, pp. 020012-1-020012-8
Pub. date	2018, 1
Note	This article may be downloaded for personal use only. Any other use requires prior permission of the author and AIP Publishing. This article appeared in AIP Conference Proceedings, Vol. 1929, 1, pp. 020012-1-020012-8 and may be found at http://dx.doi.org/10.1063/1.5021925.

Fabrication and characterization of perovskite solar cells added with $MnCl_2$, YCl_3 or poly(methyl methacrylate)

Masaya Taguchi, Atsushi Suzuki, Hiroki Tanaka, and Takeo Oku

Citation: AIP Conference Proceedings **1929**, 020012 (2018); doi: 10.1063/1.5021925
View online: https://doi.org/10.1063/1.5021925
View Table of Contents: http://aip.scitation.org/toc/apc/1929/1
Published by the American Institute of Physics

Fabrication and Characterization of Perovskite Solar Cells added with $MnCl_2$, YCl_3 or Poly(methyl methacrylate)

Masaya Taguchi, Atsushi Suzuki*, Hiroki Tanaka and Takeo Oku

Department of Materials Science, The University of Shiga Prefecture,
2500 Hassaka, Hikone, Shiga 522-8533, Japan

*e-mail: suzuki@mat.usp.ac.jp

Abstract. Perovskite-type $CH_3NH_3PbI_3$-based photovoltaic devices were fabricated and characterized. Effects of manganese (Mn), yttrium (Y) compounds addition into the perovskite crystal on the photovoltaic properties were investigated. Also, the effects of poly(methyl methacrylate) (PMMA) addition on perovskite layer on the photovoltaic properties were investigated. When 3 % $MnCl_2$ was added, the short circuit current density and conversion efficiency were improved by promoting the crystal growth of perovskite phase. The photoelectric conversion efficiency for 0.9 mg mL^{-1} PMMA added was 7.36 %. Open circuit voltage and fill factor were improved by 5 % YCl_3 addition.

INTRODUCTION

Perovskite solar cells (PSCs) have been the most promising devices towards the renewable energy generation recently, whose highest efficiency, 21.1 %, was achieved in 2016. In addition to their efficient light absorption and high carrier mobility, they are semiconductors with adjustable band gaps, which have the benefits to absorb different wavelengths of light and to fit into the solar devices well [1-9]. Further control over the optical and magnetic properties of quantum dots can be achieved through doping of transition metal ions such as Mn^{2+} or Co^{2+} [10]. Doping Mn^{2+} ions in a low-dimensional semiconductor nanocrystal in the quantum confinement regime provides fascinating optical, magneto-optical, and light harvesting properties mainly because of the interaction of quantum confined charge carriers of the host with the dopant ions [11].

The purpose of the present work is to investigate photovoltaic properties of photovoltaic devices with perovskite –type $MAPb_{1-x}Mn_xI_{3-2x}Cl_{2x}$, $MAPb_{1-x}Y_xI_{3-3x}Cl_{3x}$ and $MAPbI_3$/ poly(methyl methacrylate) (PMMA) (x mg mL^{-1}) compounds prepared by a simple spin-coating technique in air. Manganese chloride ($MnCl_2$) or yttrium chloride (YCl_3) is expected to work as a suitable adding material at the sites of Pb and I. Effects of $MnCl_2$ or YCl_3 addition into the perovskite crystal and PMMA addition on perovskite layer on the photovoltaic properties and microstructures were investigated using light-induced current density voltage (*J-V*) curves, incident photon to conversion efficiency (IPCE), X-ray diffraction (XRD), optical microscopy (OM) and scanning electron microscopy (SEM) equipped with energy dispersive spectroscopy (EDS).

EXPERIMENTAL

A schematic illustration of the fabrication process of the present $MAPb_{1-x}Mn_xI_{3-2x}Cl_{2x}$, $MAPb_{1-x}Y_xI_{3-3x}Cl_{3x}$ and $MAPbI_3$/ PMMA (x mg mL^{-1}) photovoltaic cells is shown in Fig. 1. The detailed fabrication process was described in the previous reports [12-14]. F-doped tin oxide (FTO) substrates were cleaned using an ultrasonic bath with acetone and methanol, and dried under nitrogen gas. 0.15 M and 0.30 M TiO_x precursor solutions were prepared from titanium diisopropoxide bis (acetyl acetonate) (Sigma Aldrich, 0.055 mL and 0.11 mL) with 1-butanol (Nacalai Tesque, 1 mL).

The Irago Conference 2017
AIP Conf. Proc. 1929, 020012-1–020012-8; https://doi.org/10.1063/1.5021925
Published by AIP Publishing. 978-0-7354-1621-5/$30.00

The 0.15 M TiO_x precursor solution was spin-coated on the FTO substrate at 3000 rpm for 30 s and annealed at 125 °C for 5 min. This process of 0.30 M solution was performed twice, and the FTO substrate was sintered at 500 °C for 30 min to form a compact TiO_2 layer. After that, TiO_2 paste was coated on the substrate by spin-coating at 5000 rpm for 30 s. For the mesoporous TiO_2 layer, the TiO_2 paste was prepared with TiO_2 powder (Aerosil, P-25) with poly (ethylene glycol) (Nacalai Tesque, PEG #20000) in ultrapure water [15]. The solution was mixed with acetylacetone (Wako Pure Chemical Industries, 10 μL) and triton X-100 (Sigma Aldrich, 5 μL) for 30 min, and was left for 24 h to suppress the bubble in the solution. The cells were annealed at 125 °C for 5 min and at 500 °C for 30 min to form the mesoporous TiO_2 layer [16]. For the preparation of the perovskite compounds added with transition metal elements, solutions of CH_3NH_3I (Tokyo Chemical Industry), PbI_2 (Sigma Aldrich) with $MnCl_2$ (Sigma Aldrich) or YCl_3 (Sigma Aldrich) with a desired mole ratio in γ-butyrolactone (Wako Pure Chemical Industries, 0.3 mL) and N,N-dimethylformamide (Sigma Aldrich, 0.2 mL) was mixed at 60 °C at 24 h. Table 1 shows preparation compositions of the perovskite phases. Solutions of the perovskite phases were then introduced into the TiO_2 mesopores by spin-coating at 2000 rpm for 60 s and annealed at 100 °C for 15 min. Then , a hole transport layer (HTL) was prepared by spin-coating at 4000 rpm for 30 s. As the HTL, a solution of 2,2',7,7'-tetrakis- (N,N-di-p-methoxyphenylamine)-9,9'-spirobifluorene (Spiro-OMeTAD, Sigma Aldrich, 36.1 mg) in chlorobenzene (Wako Pure Chemical Industries, 0.5 mL) was mixed with a solution of lithium bis (trifluoromethylsulfonyl) imide (Li-TFSI, Tokyo Chemical Industry, 260 mg) in acetonitrile (Sigma Aldrich, 0.5 mL) for 24 h. The former solution with 4-tertbutylpyridine (Sigma Aldrich, 14.4 μL) was mixed with the Li-TFSI solution (8.8 μL) for 30 min at 70 °C. All procedures were carried out in ordinary air. Finally, gold (Au) electrodes were evaporated as top electrodes [17]. Layered structures of the present photovoltaic cells are denoted as FTO/TiO_2/perovskite/spiro-OMeTAD/Au, as shown in a schematic illustration of Fig. 1.

For the preparation of the perovskite compounds added with PMMA on perovskite layer, solutions of CH_3NH_3I (Tokyo Chemical Industry, 190.7 mg), $PbCl_2$ (Sigma Aldrich, 111.2 mg) with a desired mole ratio in N,N-dimethylformamide (Sigma Aldrich, 0.5 mL) was mixed at 60 °C at 24 h. Solutions of the perovskite phases were then introduced into the TiO_2 mesopores in a dry air flow by spin-coating at 2000 rpm for 60 s and annealed at 140 °C for 10 min. For the preparation PMMA solutions, PMMA(Sumitomo Chemical) solution with different concentrations from the mixed solvent of chlorobenzene (Wako Pure Chemical Industries) and toluene(Wako Pure Chemical Industries) (volume ratio of chlorobenzene and toluene is 9:1) was pipetted onto the perovskite layer by spin-coating at 4000 rpm for 30 s and annealed at 100 °C for 15 min [18]. Then, a hole transport layer (HTL) was prepared by spin-coating at 4000 rpm for 30 s. As the HTL, a solution of 2,2',7,7'-tetrakis- (N,N-di-p-methoxyphenylamine)-9,9'-spirobifluorene (Spiro-OMeTAD, Sigma Aldrich, 36.1 mg) in chlorobenzene (Wako Pure Chemical Industries, 0.5 mL) was mixed with a solution of lithium bis (trifluoromethylsulfonyl) imide (Li-TFSI, Tokyo Chemical Industry, 260 mg) in acetonitrile (Sigma Aldrich, 0.5 mL) for 24 h. The former solution with 4-tertbutylpyridine (Sigma Aldrich, 14.4 μL) was mixed with the Li-TFSI solution (8.8 μL) for 30 min at 70 °C. All procedures were carried out in ordinary air. Finally, gold (Au) electrodes were evaporated as top electrodes. Layered structures of the present photovoltaic cells are denoted as FTO/TiO_2/perovskite/PMMA/spiro-OMeTAD/Au, as shown in a schematic illustration of Fig. 1.

The *J-V* characteristics (KEYSIGHT B2901A) of the photovoltaic cells were measured under illumination at 100 mW cm^{-2} by using an AM 1.5 solar simulator (San-ei Electric XES-301S). The solar cells were illuminated through the side of the FTO substrates, and the measurement area was 0.090 cm^2. The IPCE of the cells was also investigated for the same samples (Enli Technology, QE-R). The microstructures of the perovskite layers were investigated by using an X-ray diffractometer (Bruker, D2 PHASER), an optical microscope (Nikon, Eclipse E600) and a scanning electron microscope (Jeol, JSM-6010PLUS/LA).

TABLE 1. Preparation composition of the present perovskite solar cells.

	Additive composition ratio (%)	
Preparation composition	PbI_2 : $MnCl_2$	PbI_2 : YCl_3
$MAPbI_3$		
$MAPb_{0.97}Mn_{0.03}I_{2.94}Cl_{0.06}$	97 : 3	-
$MAPb_{0.95}Mn_{0.05}I_{2.90}Cl_{0.10}$	95 : 5	-
$MAPb_{0.93}Mn_{0.07}I_{2.86}Cl_{0.14}$	93 : 7	-
$MAPb_{0.97}Y_{0.03}I_{2.91}Cl_{0.09}$	-	97 : 3
$MAPb_{0.95}Y_{0.05}I_{2.85}Cl_{0.15}$	-	95 : 5
$MAPb_{0.90}Y_{0.10}I_{2.70}Cl_{0.30}$	-	90 : 10

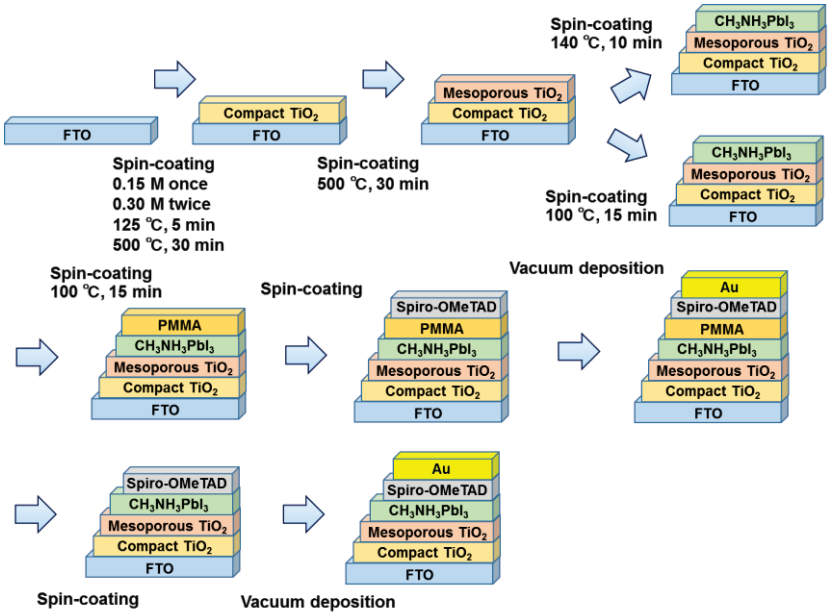

FIGURE 1. Schematic illustration of fabrication process of the present photovoltaic devices.

RESULTS AND DISCUSSION

J-V characteristics of the FTO/TiO_2/perovskite/spiro-OMeTAD photovoltaic cells under illumination are shown in Fig. 2, which indicates an effect of Mn or Y addition to the $CH_3NH_3PbI_3$. Measured photovoltaic parameters of the $MAPbI_3$, $MAPb_{1-x}Mn_xI_{3-2x}Cl_{2x}$ and $MAPb_{1-x}Y_xI_{3-3x}Cl_{3x}$ cells are summarized in Table 2. In Fig. 2, the $MAPbI_3$ cell provided the conversion efficiency (η) of 2.12 %, the fill factor (*FF*) of 0.617, the short circuit current density (J_{sc}) of 4.07 mA cm^{-2} and the open circuit voltage (V_{oc}) of 0.844 V. When the 3 % $MnCl_2$ was added, the short circuit current density and the conversion efficiency were improved. When the 5 % YCl_3 was added, the open circuit voltage, the fill factor and the conversion efficiency were improved. As a result, the short circuit current densities were improved by the $MnCl_2$ or YCl_3 adding to $MAPbI_3$.

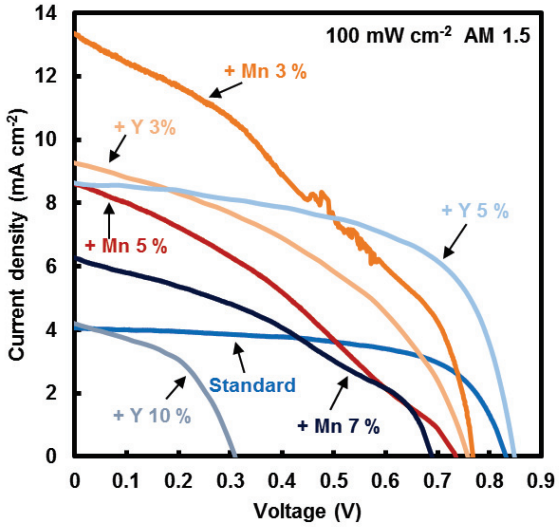

FIGURE 2. *J-V* characteristics of $MAPb_{1-x}Mn_xI_{3-2x}Cl_{2x}$ and $MAPb_{1-x}Y_xI_{3-3x}Cl_{3x}$.

TABLE 2. Measured photovoltaic parameters of $MAPb_{1-x}Mn_xI_{3-2x}Cl_{2x}$ and $MAPb_{1-x}Y_xI_{3-3x}Cl_{3x}$ cells.

$MAPb_{1-x}Mn_xI_{3-2x}Cl_{2x}$	J_{sc} (mA cm^{-2})	V_{oc} (V)	FF	η (%)
0	4.07	0.844	0.617	2.12
0.03	13.36	0.760	0.390	3.97
0.05	8.60	0.730	0.331	2.08
0.07	6.28	0.690	0.376	1.63
$MAPb_{1-x}Y_xI_{3-3x}Cl_{3x}$				
0.03	9.27	0.757	0.416	2.92
0.05	8.63	0.847	0.595	4.35
0.10	4.19	0.308	0.474	0.613

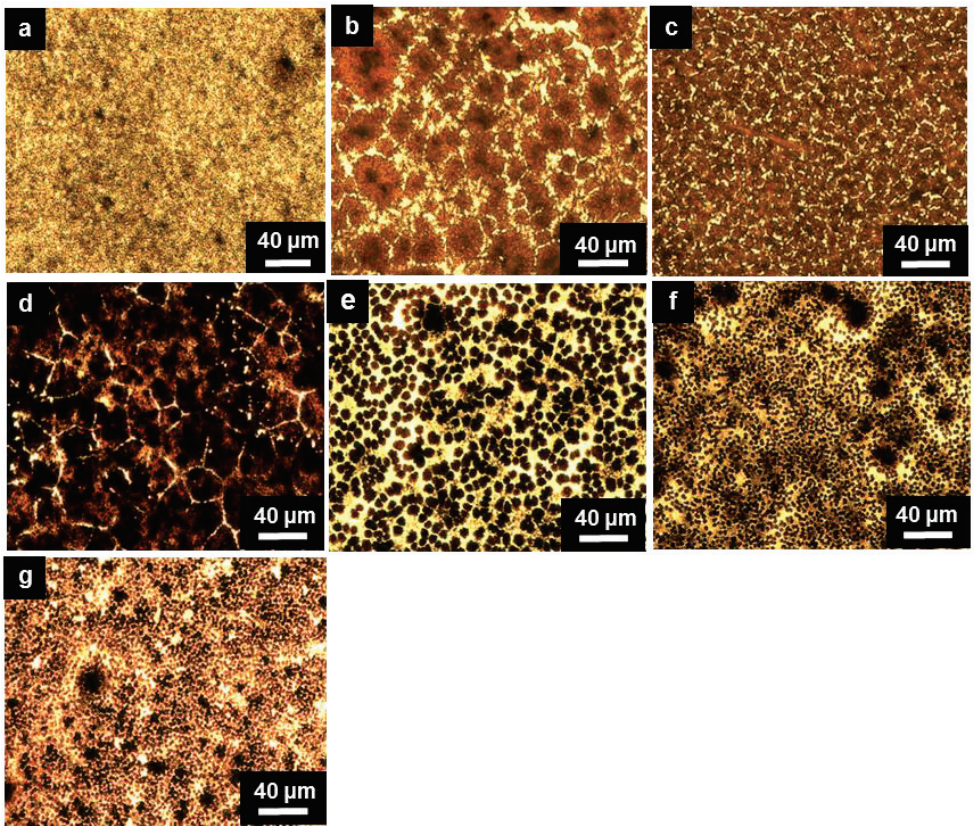

FIGURE 3. Optical microscope images of solar cells base on the following perovskite phase : (a) $MAPbI_3$, (b) $MAPb_{0.97}Mn_{0.03}I_{2.94}Cl_{0.06}$, (c) $MAPb_{0.95}Mn_{0.05}I_{2.90}Cl_{0.10}$, (d) $MAPb_{0.93}Mn_{0.07}I_{2.86}Cl_{0.14}$, (e) $MAPb_{0.97}Y_{0.03}I_{2.91}Cl_{0.09}$, (f) $MAPb_{0.95}Y_{0.05}I_{2.85}Cl_{0.15}$, (g) $MAPb_{0.90}Y_{0.10}I_{2.70}Cl_{0.30}$.

Optical microscope images of the present $MAPbI_3$ added with $MnCl_2$ or YCl_3 photovoltaic cells are shown in Fig. 3 (a)-(g). In the cells to which $MnCl_2$ was added, the crystal growth was entirely promoted. In particular, the crystal growth of the cell to which 3 % $MnCl_2$ was added was most notably observed. When the 5 % YCl_3 was added, the crystal became dense.

XRD patterns of $MAPbI_3$ and $MAPb_{1-x}Mn_xI_{3-2x}Cl_{2x}$ photovoltaic cells are shown in Fig. 4. Formation of PbI_2 was suppressed by $MnCl_2$ addition.

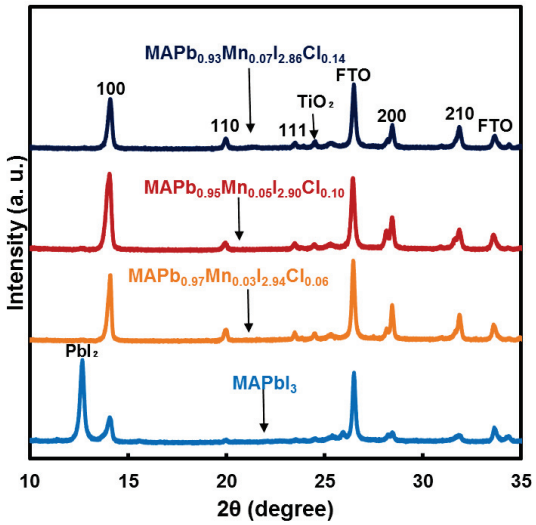

FIGURE 4. XRD patterns of $MAPbI_3$ and $MAPb_{1-x}Mn_xI_{3-2x}Cl_{2x}$ photovoltaic cells.

J-V characteristics of the FTO/TiO_2/perovskite/PMMA/spiro-OMeTAD photovoltaic cells under illumination are shown in Fig. 5 (a), which indicates an effect on PMMA addition on the perovskite layer. Measured photovoltaic parameters of the $MAPbI_3$/ PMMA (x mg mL^{-1}) perovskite solar cells are summarized in Table 2. IPCE spectra of FTO/TiO_2/perovskite/PMMA/spiro-OMeTAD/Au cells are shown in Fig. 5 (b). In Fig. 5 (a), the $MAPbI_3$ cell provided the conversion efficiency (η) of 1.94 %, the fill factor (*FF*) of 0.235, the short circuit current density (J_{sc}) of 14.51 mA cm^{-2} and the open circuit voltage (V_{oc}) of 0.569 V. When the 0.9 mg mL^{-1} PMMA was added on the perovskite layer, J_{sc}, V_{oc}, *FF* and η were improved. The perovskite solar cells added with 0.9 mg mL^{-1} PMMA showed the highest conversion efficiency of 7.36 %. In Fig. 5 (b), the short circuit current density and the external quantum efficiency were correlated.

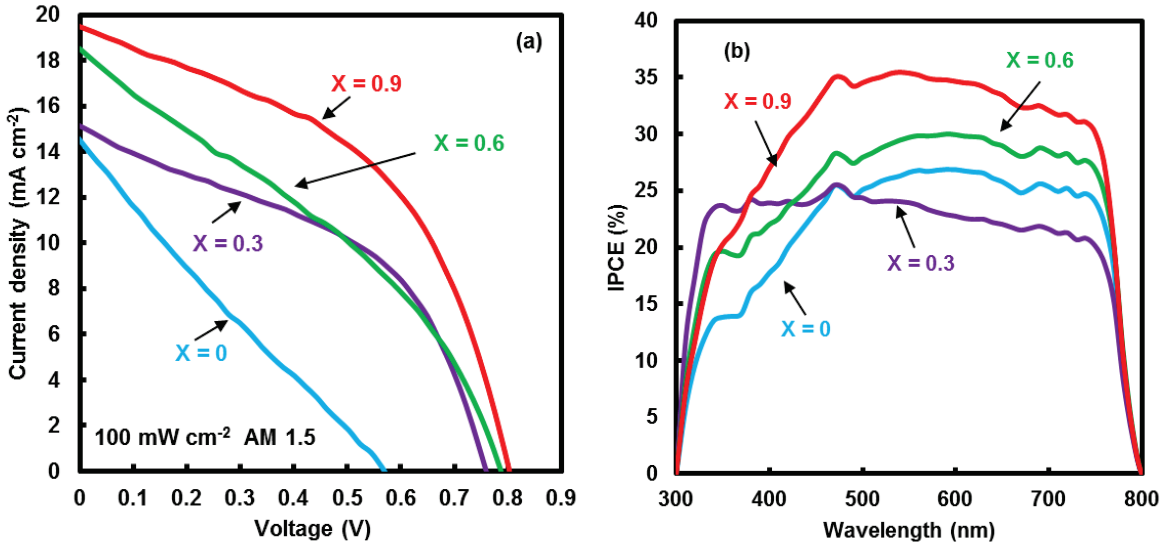

FIGURE 5. (a) *J-V* characteristics and (b) IPCE spectra of the $MAPbI_3$/ PMMA (x mg mL^{-1}) perovskite solar cells.

TABLE 3. Measured photovoltaic parameters of $MAPbI_3$/ PMMA (x mg mL^{-1}) perovskite solar cells.

x (mg mL^{-1})	J_{sc} (mA cm^{-2})	V_{oc} (V)	*FF*	η (%)
0	14.51	0.569	0.235	1.94
0.3	15.14	0.759	0.453	5.20
0.6	18.47	0.787	0.347	5.04
0.9	19.50	0.803	0.470	7.36

Optical microscope images of $MAPbI_3$/ PMMA (x mg mL^{-1}) perovskite solar cells are shown in Fig. 6 (a)-(d). When 0.9 mg mL^{-1} PMMA was added on the perovskite layer, crystal growth was promoted. It is considered that promotion of crystal growth contributed to improvement of conversion efficienty. On average, the size of the crystals was about 10 to 20 μm, and crystals of 30 μm existed as large ones.

Fig. 7 (a)-(d) are SEM images of $MAPbI_3$/ PMMA (x mg mL^{-1}) perovskite solar cells. In the system to which 0.3 mg mL^{-1} PMMA added, the shape of the crystal changed to a needle shape, and growth was observed on the surface of the crystal. The composition ratios of elements Pb, I, Cl, and C : N were calculated from the EDS spectrum using background correction by normalizing the spectrum peaks, as listed in Table 4.

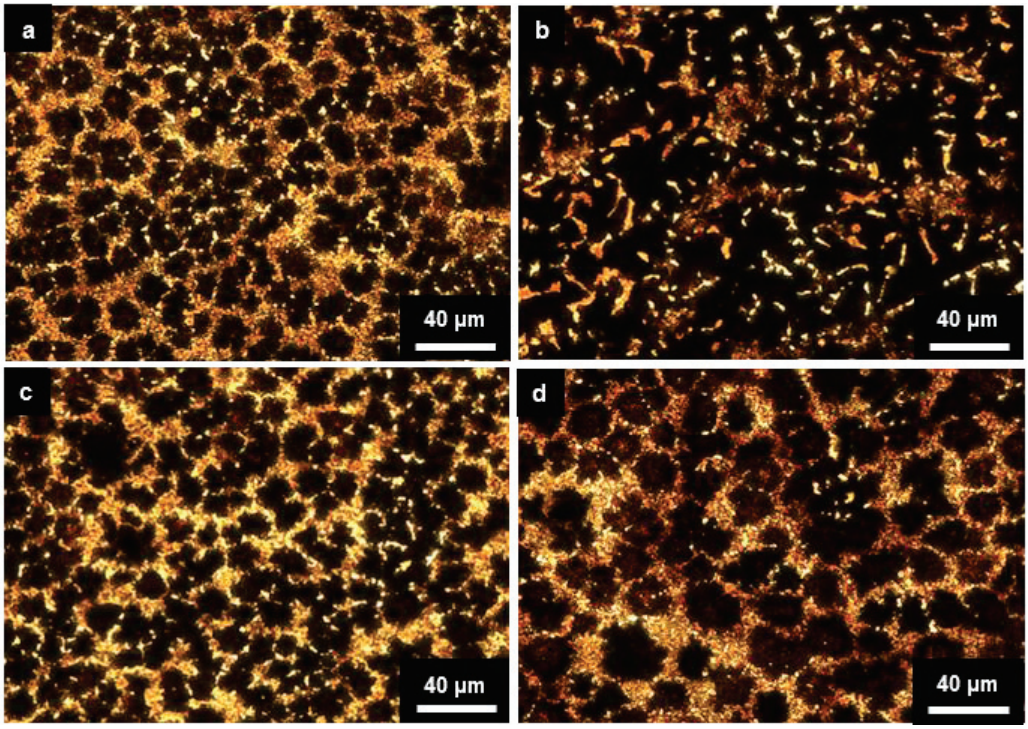

FIGURE 6. Optical microscope images of $MAPbI_3$/ PMMA (x mg mL^{-1}) perovskite solar cells. The concentration of PMMA are (a) 0 mg mL^{-1}, (b) 0.3 mg mL^{-1}, (c) 0.6 mg mL^{-1}, (d) 0.9 mg mL^{-1}.

When $MnCl_2$ was added, improvement in short circuit current density was confirmed. This is believed to be due to the contribution of crystal growth promotion of the perovskite phase and suppression of formation of PbI_2, which contributies to better quality of perovskite crystals and reduced charge recombination. The crystal became dense, and the short circuit current density was improved by YCl_3 addition. By adding PMMA, the crystal size increases, and the charge loss is reduced. Therefore, short circuit current density and open circuit voltage we are improved.

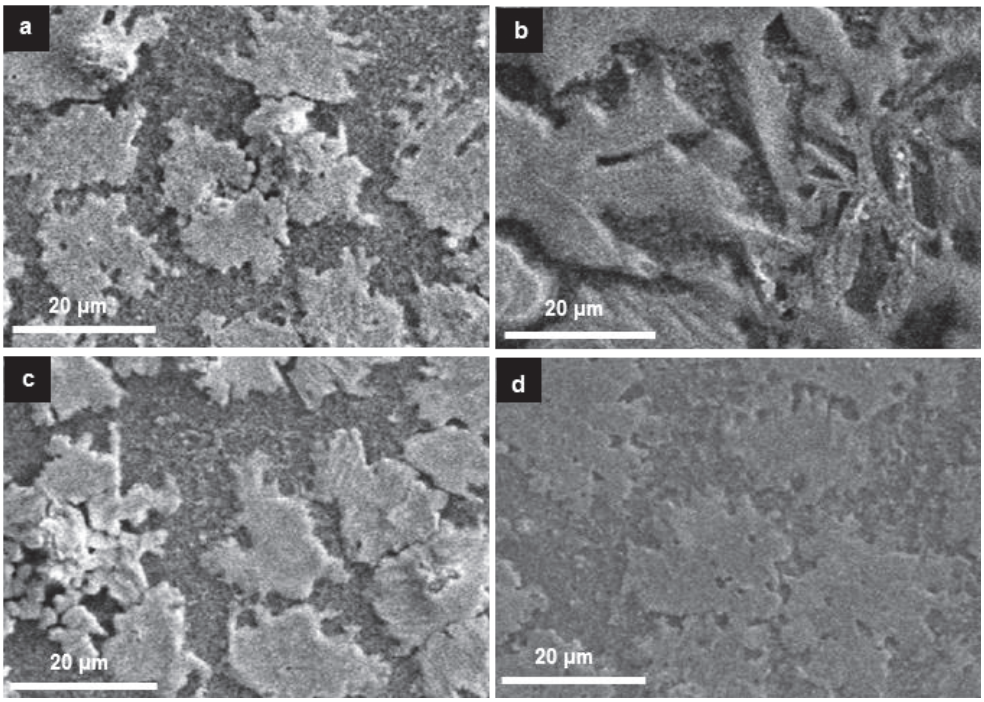

FIGURE 7. SEM images of $MAPbI_3$/ PMMA (x mg mL^{-1}) perovskite solar cells. The concentration of PMMA are (a) 0 mg mL^{-1}, (b) 0.3 mg mL^{-1}, (c) 0.6 mg mL^{-1}, (d) 0.9 mg mL^{-1}.

TABLE 4. Measured compositions of $MAPbI_3$/ PMMA (x mg mL^{-1}) perovskite solar cells.

PMMA (mg mL^{-1})	Pb (at.%)	I (at.%)	Cl (at.%)	C : N (at.%)
0	36.5	58.3	5.2	56.7 : 43.3
0.9	33.4	61.8	4.8	50.0 : 50.0

CONCLUSION

The perovskite-based solar cells were fabricated by a spin-coating method, and effects of $MnCl_2$ or YCl_3 addition to the perovskite and PMMA addition on perovskite layer on the photovoltaic properties were investigated. By adding 3 % $MnCl_2$, crystal growth was promoted and the short circuit current density and the conversion efficiency were improved. Formation of PbI_2 was suppressed by $MnCl_2$ addition. The open circuit voltage, fill factor and conversion efficiency were improved by 5 % YCl_3 addition. The surface structures of the devices were investigated by optical microscopy. The crystal became dense by 5 % YCl_3 addition. The perovskite solar cells added with 0.9 mg mL^{-1} PMMA showed the highest conversion efficiency of 7.36 %. The IPCE were investigated by spectral sensitivity measurement, which indicated that the short circuit current density and the IPCE were correlated. In the system to which 0.3 mg mL^{-1} PMMA added, the shape of the crystals changed to a needle shape, and growth was observed on the surface of the crystal.

REFERENCES

1. B. Nafradi, P. Szirmai, M. Spina, H. Lee, O. V. Yazyev, A. Arakcheeva, D. Chernyshov, M. Gibert, L. Forro, and E. Horvath, Nat. Comm, **7**, 13406 (2016).
2. P. Umari, E. Mosconi, and F. D. Angelis, Sci. Rep., **4**, 4467 (2014).
3. T. Zhao, W. Shi, J. Xi, D. Wang, and Z. Shuai, Sci. Rep., **6**, 19968 (2016).
4. Y. Y. Pan, Y. H. Su, C. H. Hsu, L. W. Huang, K. P. Dou, and C. C. Kaun, Nanomaterials, **1**, 33-38 (2016).
5. N. Li, Z. Zhu, C. C. Chueh, H. Liu, B. Peng, A. Petrone, X. Li, L. Wang, and A. K. Y. Jen, Adv. Energy. Mater., **7**, 1601307 (2017).
6. D. Cortecchia, H. A. Dewi, J. Yin, A. Bruno, S. Chen, T. Baikie, P. P. Boix, M. Gratzel, S. Mhaisalkar, C. Soci, and N. Mathews, Inorg. Chem., **55**, 1044-1052 (2016).
7. T. Oku, Y. Ohishi, A Suzuki, and Y. Miyazawa, J. Ceram. Soc. Jpn., **125**, 303-307 (2017).
8. X. Zhang, J. Yin, Z. Nie, Q. Zhang, N. Sui, B. Chen, Y. Zhang, K. Qu, J. Zhao, and H. Zhou, RSC. Adv, **7**, 37419-37425 (2017).
9. F. Wang, A. Shimazaki, F. Yang, K. Kanahashi, K. Matsuki, Y. Miyauchi, T. Takenobu, A. Wakamiya, Y. Murata, and K. Matsuda, J. Phys. Chem. C, **121**, 1562-1568 (2017).
10. C. C. Lin, K. Y. Xu, D. Wang, and A. Meijerink, Sci. Rep., **7**, 45906 (2017).
11. W. J. Mir, M. Jagadeeswararao, S. Das, and A. Nag, ACS. Energy. Lett., **2**, 537-543 (2017).
12. T. Oku, Y. Ohishi, A. Suzuki, and Y. Miyazawa, Metals, **6**, 147 (2016).
13. M. Zushi, A. Suzuki, T. Akiyama, and T. Oku, Chem. Lett, **43**, 916 (2014).
14. T. Oku, M. Zushi, Y. Imanishi, A. Suzuki, and K. Suzuki, Appl. Phys. Express, **7**, 121601 (2014).
15. T. Oku, N. Kakuta, K. Kobayashi, A. Suzuki, and K. Kikuchi, Prog. Nat. Sci. Mater. Int., **21**, 122 (2011).
16. T. Oku, K. Suzuki, and A. Suzuki, J. Ceram. Soc. Jpn., **124**, 234 (2016).
17. N. Ueoka, Y. Ohishi, Y. Shirahata, A. Suzuki, and T. Oku, AIP Conf. Proc, **1807**, 020009 (2017).
18. D. Bi, C. Yi, J. Luo, J. D. Decoppet, F. Zhang, S. M. Zakeeruddin, X. Li, A. Hagfeldt, and M. Gratzel, Nat. Energy, **1**, 16142 (2016).